Advances in Social Sciences and Management
July 2023, Vol-1, No-7, pp. 16-45

On the Origin and Generation Mechanism of Large-Scale Vortices in Tidal Estuaries

Takeo R. M. Nakagawa[1] and Ai Nakagawa[2]

1. Institute of Environmental Fluid Mechanics, Advanced College of Symbiosis Hakusan
2. Department of Environmental Sciences, Academy of Hakusan 2-14, Hakusan 920-2152 Japan

Abstract:
Large scale vortices in strong tidal currents have been found on the tranquil sea surface at Western Port, Melbourne, Australia. It is found by the similitude analyses that the origin and generation mechanism of these vortices are governed by the following relation: d/$\boldsymbol{\delta}$ = Ж ($|a|$/g, UD/ν), where d is the diameter of vortices, $\boldsymbol{\delta}$ the scale of dunes, $|a|$ the absolute value of acceleration and/or deceleration of tidal current, g the gravitational acceleration, U the velocity of tidal current, D the depth of water, and ν the kinematic viscosity of the sea water. Note Ж is an unknown function introduced by the analyses. Aerial observation of dye patches reveals sometimes remarkably regular honeycomb arrangement in a manner in which they are distributed over the sea surface. In the field, flow visualization by two color dye patches, and sea bed survey in terms of a side-scan sonar have been done, while in the laboratory, extensive towing experiments have been conducted to demonstrate the constant, accelerated and/or decelerated flows over each dune model for simulating cycle of tidal currents. On the basis of field and laboratory experiments, the nature, origin, and generation mechanism of the vortices are scrutinized. In general, it is possible that vortices on the sea surface have various origins such as thermal convection (Bénard cell) and wind shear stress (Langmuir cell). Contrary to these ordinary origins of vortices, it has been concluded that they are generated by the interaction of tidal currents and sand dunes at singular time during spring tide: When tidal currents change from acceleration to deceleration, the fluid body in the re-circulatory flow region (cavity) behind each dune crest is intensified during the acceleration period, and then it is ejected upwards and changed into a pair of vortices. Then, the paired vortices are transported to the sea surface in experiencing a series of change in the structure, and finally form the cellular vortices on the sea surface, with which diameter of each vortex is increased by the interaction. It is inferred that this new finding is critical to understand any oscillating flow over the roughness with the separation in nature and laboratory accompanying the cyclical change from acceleration to deceleration and vice versa.

Keywords: Hydraulics & hydrodynamics, In situ testing, Laboratory tests, Mechanisms, Models(physical), Shallow water.

INTRODUCTION

Over the last half-century, it has been known by fishermen, seamen, oceanographers and others in Australia, Japan, USA, Italy, UK, and/or Norway that intriguing vortices (or boils) similar to Bénard cell appear on the tranquil water surface of estuaries and/or rivers. (Pollock 1973, Kostaschuk et al. 1993, Ckadel et al. 2009,Talke et al. 2013, Branch et al. 2021) together with on the surface of water channelsin laboratory (Müller et al. 1986, Nezu & Nakagawa 1993, Yue et al. 2005, Mandel etal. 2017, Gakhar e al. 2020).

This enhances us to investigate into those vortices at Western Port, Australia.

Observation made during dye release has shown the existence of large-scale vorticesin strong tidal currents as shown in Fig.1(a). These observations, made in tidal estuaries in Western Port, Australia by Hinwood and his students (Pollock 1973; Chandler & Berzkalns 1977, Nakagawa & Hinwood 1978, Hinwood 1978, Nakagawa 1979a) have been extended by the study of aerial photographs of bays and tidal inletsin other Australian States, Delaware Bay, U.S.A, Naruto Strait in Seto-inland Sea, Japan as shown in Fig.1(b) and so forth. These vortices were coined by anonymous Japanese as 'Uzushio' (Tidal Vortex, 渦潮) in earlier than the tenth-century: In thehistorical book, named "Tosa Nikki", Tsurayuki Kino (1912) referred to "Uzushio" observed during his journey in 935 returning to Kyoto from Tosa province across theNaruto Strait. Very recently, it is realized by the authors that vortices observed at Western Port are quite similar to those at Naruto Strait in their origin and mechanismof generation. This prompts us to investigate the vortices with a renewed interest. Despite the widespread occurrence of these vortices, very little is known about their origin and mechanism of generation. It is evident that the vortices alter the rate of diffusion or dispersion of effluents within the water and may influence the rate of sediment transport and of dissipation of tidal energy, hence a sound understanding of the vortices is essential to the study of flow in estuaries and tidal inlets.

Fig.1(a) Aerial photograph of large-scale vortices in Western port,Victoria, Australia. After Pollock, 1973.

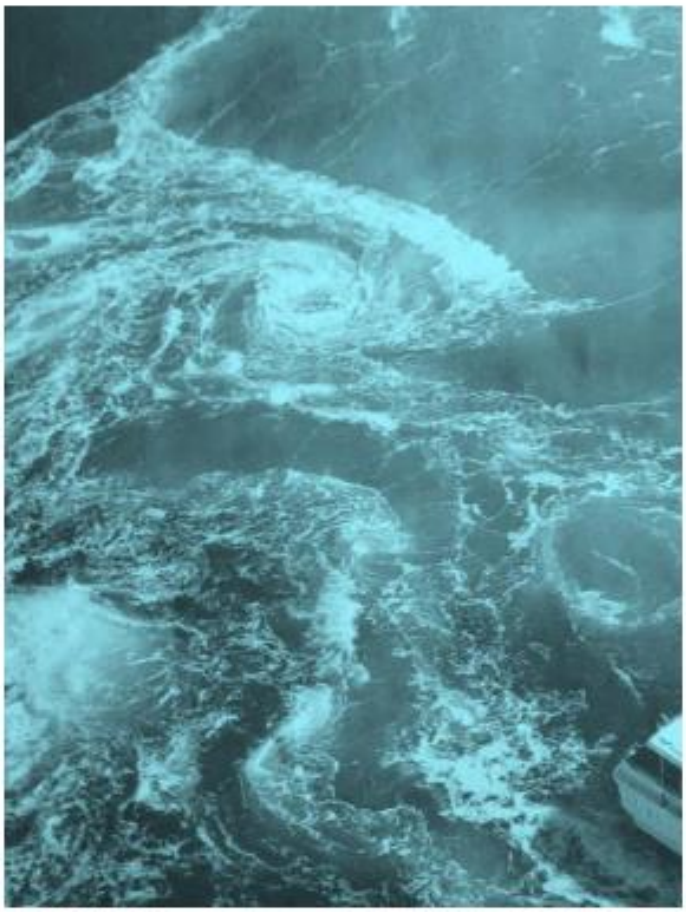

Fig.1(b) "Uzushio" in Naruto strait, Seto-inland sea, Tokushima, Japan. After the Asahi, Morning Paper, 10 March, 2018

Fig.1(a) taken by Pollock (1973) shows a group of the vortices observed on the sea surface at Western Port, Victoria, Australia. In this photograph, numerous largevortex structures are visible by sun light reflection from the sea surface, and the actualshape and size of these structures can be deduced. Dye released from the researchboat (5 m in length) is initially confined to the boundary between adjacent vortices, but subsequently is mixed into the vortices. It may also be seen that although thereare characteristic dimensions of vortex width and length these dimensions cover a range of values, with the length being typically about one-half to twice the width.

Fig.1(b) shows a group of the vortices observed on the sea surface at Naruto Straight, Seto-inland sea, Japan, where this photograph was taken from Ohnaruto bridge (length=1,929 m) through a transparent glass at 45 m high from the sea surface.It can be noticed several circular vortices on the sea surface around the boat (width≈3m).

In the present paper, based on field and laboratory experiments, a hypothesis for the mechanism of generation of the vortices in tidal inlets will be presented. This mechanism depends upon the disturbance of the tidal currents caused by the presence of dunes on the sea bed. Before mentioning this hypothesis, the observational data made in Western Port, Australia will be presented.

OBSERVATION OF VORTICES

Dye Release Experiments

Dye was released into strong tidal currents flowing in Western Port, an un-stratified tidal inlet located 55 km south-east from the center of Melbourne.

Fig. 2 Plan view of Western Port, located ca. 55 km to SE from Melbourne, Australia. Rectangle shows North Arm experiment site.Source Wikipedia (2020) Western Port Map, accessed 19 March 2020. https://en.wikepedia.org/wiki/File:western-Port_Map.PNG.

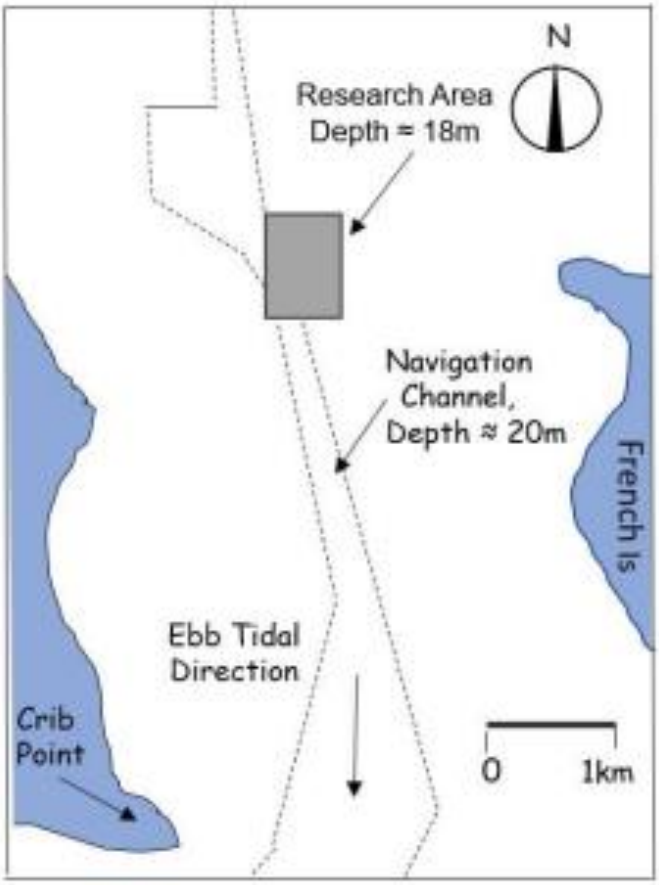

Fig.3 Detailed view of the test site.

Fig. 2 shows a plan view of Western Port, while Fig. 3 provides a detailed view of the test site. The mean water depth at the test site was 18 m.

The dye release was made during the ebb tide, with the current flowing to the southwith a speed of 0.51 m/s. Mean water temperature was14.8 ℃ and the weather was fine with a light breeze of less than 1 m/s, which caused waves of height less than 0.2m.

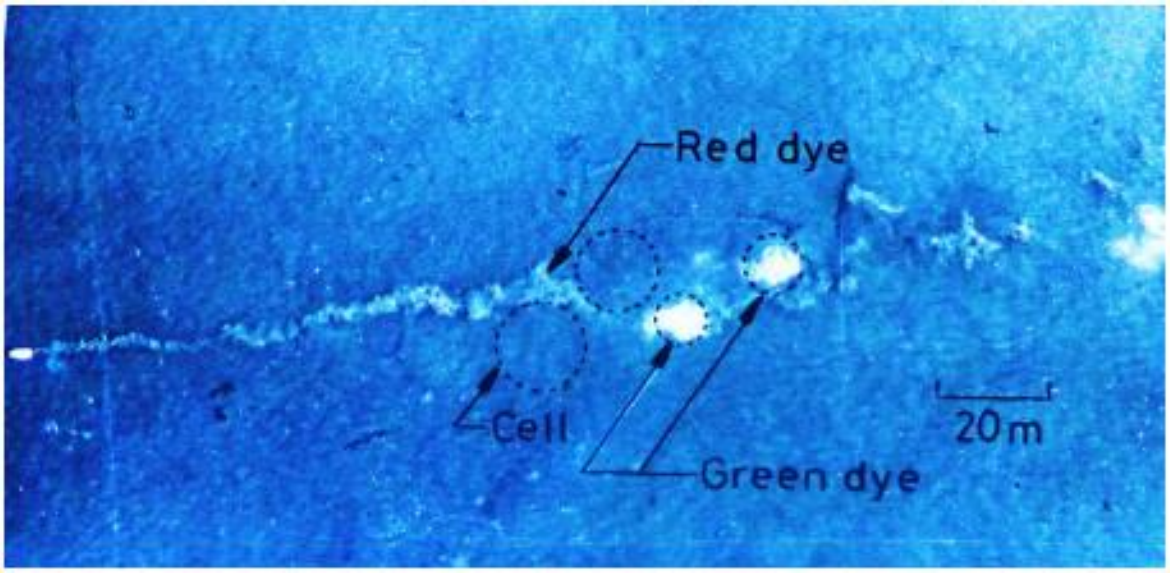

Fig.4 (a) Aerial photograph of a cellular vortex motion.

Boat length=5 m. The cells appear as lighter patches, while descending water ontheir edges is darker; red dye and green dye are shown as dark grey and white on this photograph, respectively.

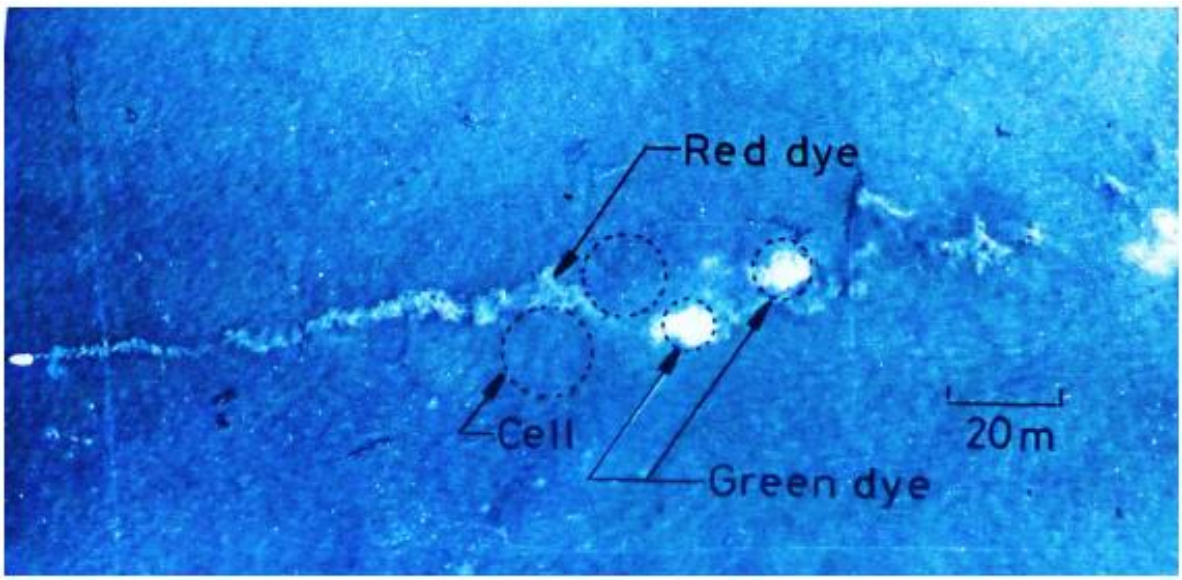

Fig. 4(b) Aerial photograph of a cellular vortex motion with telephoto lens.

Two different color dyes were released at different depths, respectively. The reddye Rhodamine was released at a depth of 2 m, while the green dye Fluorescein was released at a depth of 7 m below the sea surface. The whole water depth was approximately 18.0 m. The dyes were photographed from a light airplane flying at a height of ca. 330 m. Fig. 4(a) shows the lower green dye appearing through the center of each vortex colored by the upper red dye. This clearly indicates that there exists an upwards flow in the center of each vortex, as deduced from other data by Hinwood (1978). Fig. 4(b) shows a magnified view of part of Fig. 4(a) taken with a telephoto lens giving an effective height of 83 m.

Distribution of Vortex Diameters on Sea Surface

Chandler & Berzkalns (1977) analyzed the dye traces shown in Figure 4 and constructed distribution of vortex lengths, such as that shown in Fig. 5. To cope withthe broad range of possible vortex diameters, and the multi-valued nature of the curvewhich formed the boundary of the dye patch, they used a technique which has been often applied to meandering streams.

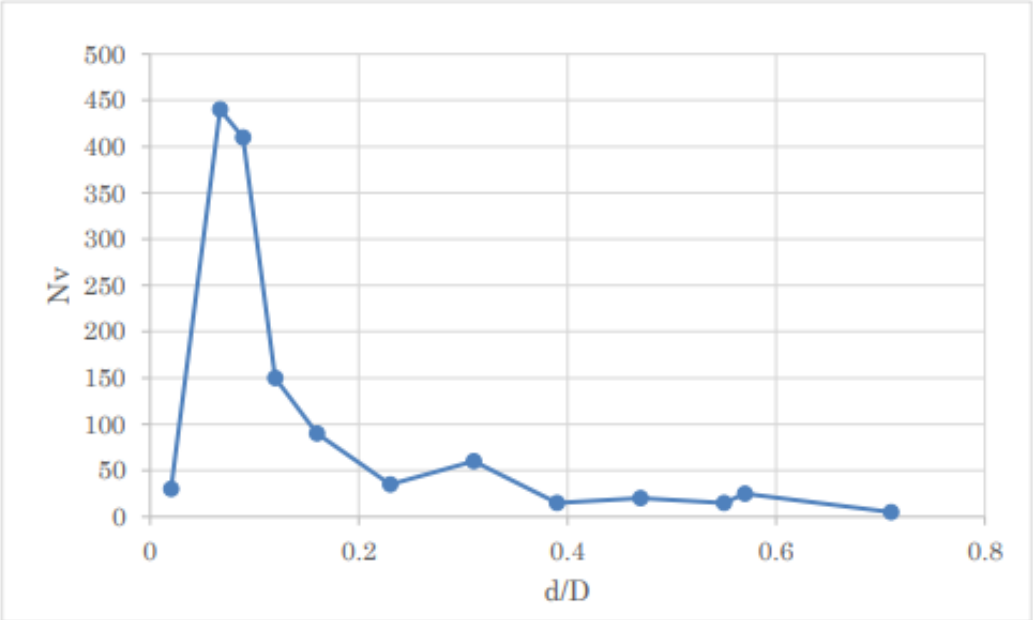

Fig. 5 Number of vortex Nv against normalized vortex diameter d/D

In Fig. 5, the ordinate denotes the number of occurrences of vortices Nv of a givensize, out of a total population of 2,636 (1,464 for red dye and 1,172 for green dye), whilethe abscissa is the normalized vortex diameter d/D as observed at the sea surface, within the range from 0.0225 to 0.706, a range limited in part by the photographic anddrafting techniques but containing the whole range of visually observable secondaryvortex motions.

Vertical Variations

Detailed vertical velocity profiles were obtained during the dye experiments, a sample of which is shown in Fig. 6. These were made using a propeller-type current-meter, integrating over a period of 30 seconds, hence it cannot provide instantaneous information about motions in the vortices but only the mean flow of a single direction. The current meter used for the present field work has 4 blades ofaxial flow propellor, mounted in a cylindrical shroud that is 80mm long in the flow direction and has an internal diameter of ca. 98mm, with clearance <1mm.

Rotations are detected by a hall-effect switch on the shroud with small magnets mounted on the tips of the vanes. Only 2 tips have magnets fitted, thus measurements are accurate to an average uncertainty of 1/2 revolution. The shroud is made of stainless steel, while the propellor itself is made of nylon, so its inertia is close to that of water; bearings are tempered steel on sapphire. The current meter is fitted with vane and weight, and is lowered to each of themeasuring points in the sea water by a supporting wire.

As may be seen in Figs.6(a) and (b), the velocity profile is that of a typical shear flow. The present observations have comfirmed that vortex motion is most active orevident at the period while velocity of the tidal current is accelerated, reaches at the maximum, or strongest, and then it is decelerated. *That is a certain period while thetidal current is fully established from the acceleration to deceleration through the flood tide, and particularly during the spring tide in Japan.* For example, Naruto- Uzushio appears during the spring tide conspicuously.

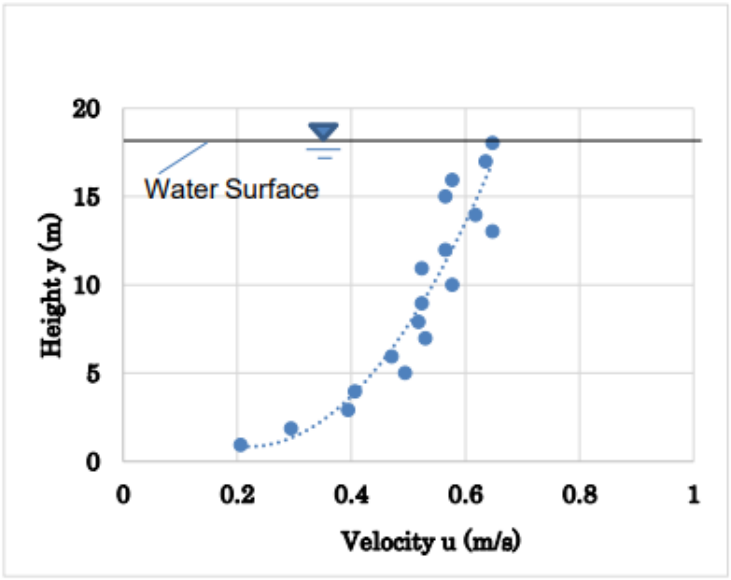

Fig. 6 (a) Height y from sea bed against tidal current velocity u.

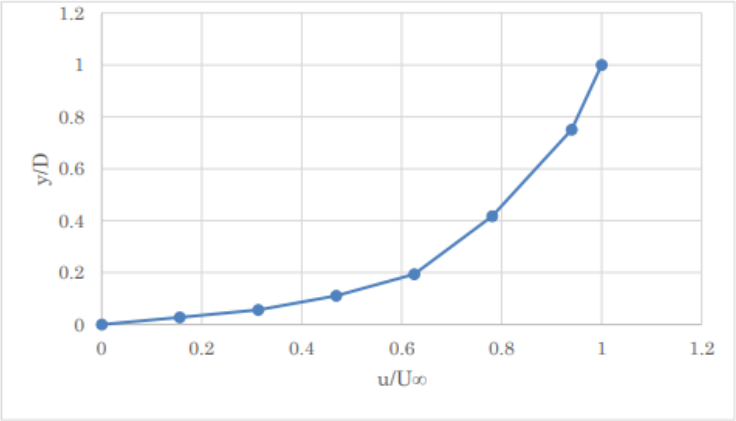

Fig.6(b) Normalized height y/D from sea bed against normalized tidalcurrent velocity u/U∞.

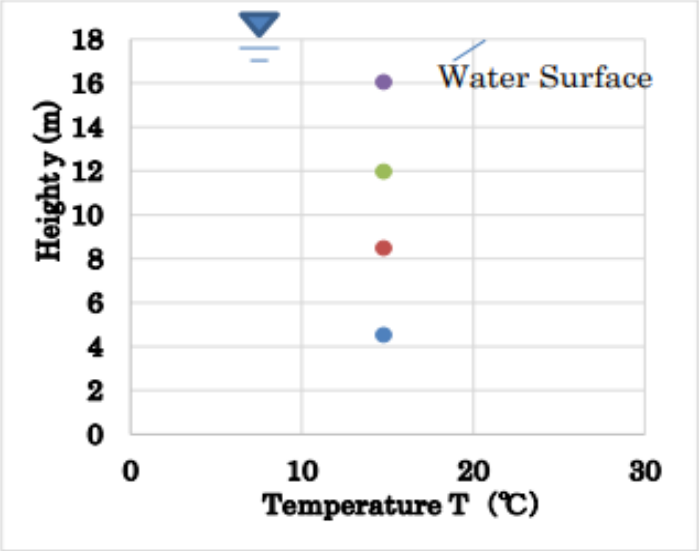

Fig.7 Height y from sea bed against water temperature T.

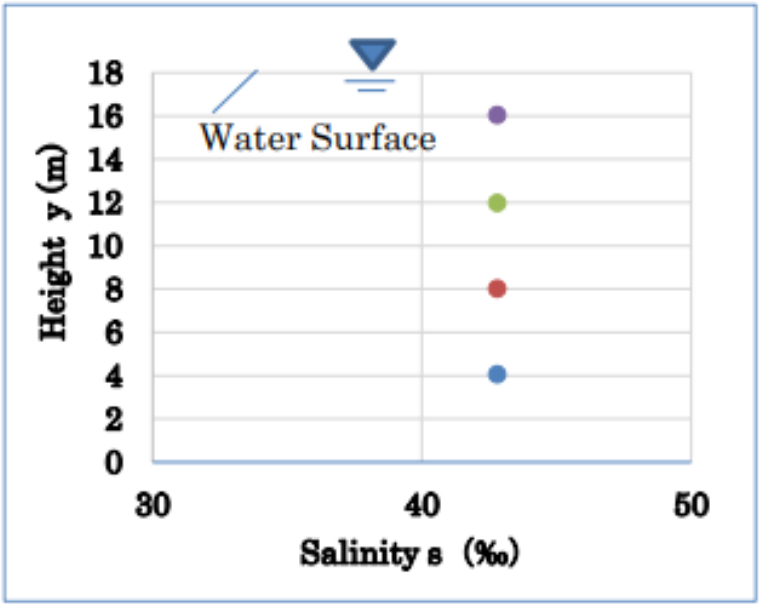

Fig. 8 Height y from sea bed against salinity s in water.

Temperature and salinity profiles are measured concurrently as the velocity profile,and are shown in Fig. 7 and Fig. 8, respectively. The temperature is uniform within 0.1℃ and the salinity within 0.01 parts per thousand, which are in fact the limits of measurement using the Hamon temperature-salinity meter, respectively. Thus, the water column is statically neutral and any instability, if any, must be of a hydrodynamicorigin.

Sea-Bed Conditions

A side-scan sonar is used to map the sea bed topography at the test area. Side-scan sonar utilizes a towed transducer array which emits sound within a perpendicular plane to the direction of towing. Echoes received from topography on the sea bed are recorded at successively greater distances from the centerline of the chartdenoting the ship's path.

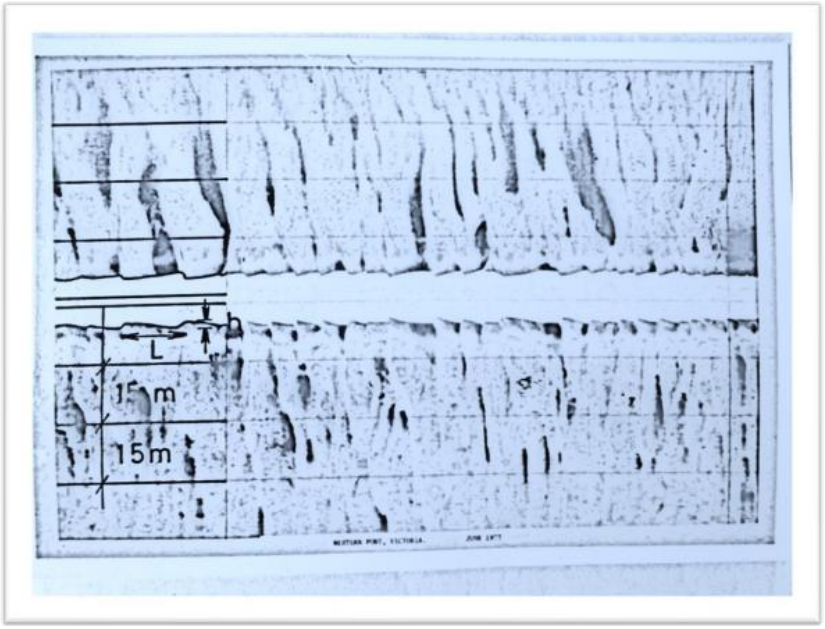

Fig. 9 Topographic photograph of the sea-bed by the side-scan sonar near the area ofdye release.

The resulting pictorial image in Fig. 9 illustrates a longitudinal profile of the sea bed beneath the tow vehicle equipped with transducer, while the trace on either side of the centerline shows the nature of topography such as sand (or mud) dunes, boulders and/or gravels on the sea bed. This figure is a portion of the side-scan sonar record for the test area, and shows a number of dunes predominantly transverseto the current direction, which coincides with that taken by the research vessel.

The scale L of the dunes is measured from the side-scan sonar charts and is foundranging from ca. 2 m to 73 m, and the steepness $\boldsymbol{\gamma}$, i.e., the ratio of height h to wavelenth L, is ranging from 0.035 to 0.19.

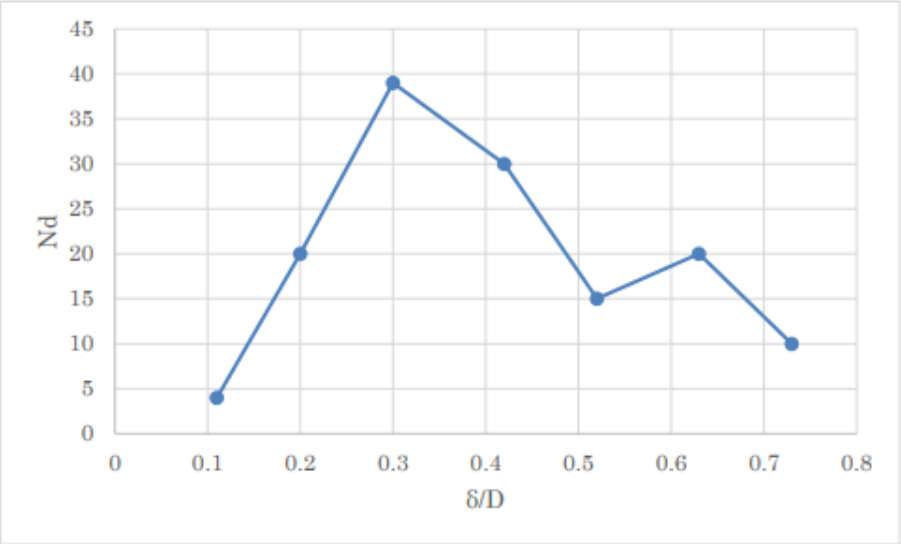

Fig. 10 Number of sand dunes Nd against the normalized sand dune scale $\boldsymbol{\delta}$/D.

Fig.10 shows a distribution of the normalized sand dune scale $\boldsymbol{\delta}$/D, where the scale $\boldsymbol{\delta}$ here is no more than the wavelength L of dune. This shows peaks at the normalized sand dune scale $\boldsymbol{\delta}$/D= 0.3. and 0.63, respectively. It may be notable that these coincide with the peaks observed in the frequency distribution of normalized vortex diameter $\boldsymbol{d}$/D in Fig.5. Although sometimes the vortices have been observedover a fairly smooth sea bed, the correspondence between the vortex diameter and the scale of sand dune on the sea bed might indicate a noticeable correlation that theinteraction of the shear flow of tidal current and sand dunes provides the favorable conditions for formation of the vortex motions observed on the sea surface in the present dye experiments. This intriguing hypothesis will be critically examined bothin the similitude analyses and in a series of laboratory experiments to be described atthe following sections, respectively.

Similitude Analyses (Zierep 1971, Zierep & Nakagawa 1986)

Let us consider the large-scale vortices appear over the sea surface in estuaryonly when the tidal flow over sand dunes on the sea bed is accelerated and then it is decelerated. It may be particularly interesting in finding the vortex diameter d on the water surface $\boldsymbol{d}$, while the tidal current is accelerating as well as decelerating. Based on the detailed observation and consideration for the present phenomena, it is realized that the vortex diameter $\boldsymbol{d}$ depends on the physical values, viz. the acceleration $|a|$ of the tidal flow, the dune scale $\boldsymbol{\delta}$ on the sea bed, the depth of water D, the mean flow velocity U, the gravitational acceleration g, the dynamic viscosity of the sea water $\boldsymbol{\mu}$, the density of the sea water $\boldsymbol{\rho}$. That is,

$$d = f\ (|a|, \delta, D, U, g, \mu, \rho\ ). \tag{1}$$

It may be evident that the more explicit relations among these physical values canbe obtained by the experiments, but such experiments must be quite difficult to complete, for there are 8 parameters in total. It is, therefore, desirable to reduce the number of the relevant parameters. For this purpose, let us select the 3 basequantities, D, U, and $\boldsymbol{\mu}$. On the other hand, the rest physical values, viz. $\boldsymbol{\sigma}$, $\boldsymbol{\delta}$, g, and $\boldsymbol{\rho}$ may be expressed by the multiple exponents, and 8−3=5 non-dimensional characteristic numbers $\boldsymbol{\pi}$i will be obtained in the following way.

At first, divide the relevant physical values into geometrical, dynamical and kinematical values as listed in Table 1.

Table 1 Summarized list of the relevant physical values

Category	Physical Value	Dimension	Symbol
Geometrical Value	Water Depth D	L	Bg
	Vortex Diameter $\boldsymbol{\sigma}$	L	A1
	Dune Scale $\boldsymbol{\delta}$	L	A2
Dynamic Value	Tidal Flow Velocity U	LT^{-1}	Bd
	Acceleration due to Gravity g	LT^{-2}	A3
	Acceleration of Tidal Flow $\|a\|$	LT^{-2}	A4
Kinematic Value	Dynamic Viscosity of Sea Water $\boldsymbol{\mu}$	$ML^{-1}T^{-1}$	Bk
	Density of Sea Water $\boldsymbol{\rho}$	ML^{-3}	A5

Referring to Table 1, write the 5 non-dimensional characteristic numbers asfollow.

$$\pi_1 = (Bg)^{x1}(Bd)^{y1}(Bk)^{z1}(A1) \tag{2}$$
$$\pi_2 = (Bg)^{x2}(Bd)^{y2}(Bk)^{z2}(A2) \tag{3}$$
$$\pi_3 = (Bg)^{x3}(Bd)^{y3}(Bk)^{z3}(A3) \tag{4}$$
$$\pi^4 = (Bg)^{x4}(Bd)^{y4}(Bk)^{z4}(A4) \tag{5}$$

and

$$\pi_5 = (Bg)^{x5}(Bd)^{y5}(Bk)^{z5}(A5). \tag{6}$$

Then, substituting the corresponding physical value for Bg, Bd, Bk, A1, A2, A3,A4, and A5 into (2), (3), (4), (5) and (6), respectively, we obtain

$$\pi_1, \pi_2, \pi_3, \pi_4, and\ \pi_5 \tag{7}$$

For example, in order to determine unknown exponents x1, y1, and z1 in (2), because the characteristic parameter $\boldsymbol{\pi}_1$ is non-dimensional by definition, we will conduct the dimensional consideration as,

$$M^0L^0T^0 = (L)^{x1}(LT^{-1})^{y1}(ML^{-1}T^{-1})^{z1}(L) = M^{z1}L^{x1+y1-z1+1}T^{-y1-z1}. \tag{8}$$

Then, comparing the exponents of the left side with those of the right side, weget

$$\pi_1 = \sigma/D. \quad (9)$$

Similarly to the above, we have

$$\pi_2 = \delta/D. \quad (10)$$
$$\pi_3 = Dg/U^2 = 1/Fr^2, with\ Fr = U/(gD)^{1/2} \quad (11)$$
$$\pi_4 = D|a|/U^2 = 1/Na^2, with\ Na = U/(|a|D)^{1/2} \quad (12)$$

and

$$\pi_5 = UD/\nu = Re, \quad (13)$$

where ν is the kinematic viscosity of the sea water.

It may be noteworthy that Fr and Re are well known Froude number and Reynolds number, respectively, while Na is the acceleration number depending on its sign whether it is positive or negative; when a is positive, the flow is accelerating, while a is negative, the flow is decelerating. It is very important to understand only when the flow is decelerating (a < $\mathbf{0}$), the vortices are generated, shed upwards and appear on the water surface if the degree of the flow deceleration is sufficiently large enough.

Hence, with (1) the following relation can be derived immediately,

$$\pi_1 = f(\pi_2, \pi_3, \pi_4, \pi_5). \quad (14)$$

Alternatively, using (9)-(13) we obtain

$$d/D = F(\delta/D, 1/Fr^2, 1/Na^2, Re). \quad (15)$$

Noting that each of characteristic parameter is non-dimensional, we can reduce number of characteristic parameters by combining π_1 and π_2 as well as $\pi_4$and π_3. Thus, we have

$$\pi_1/\pi_2 = Л(\pi_4/\pi_3, \pi_5). \quad (16)$$

Substituting (9) – (13) in (16), we obtain

$$d/\delta = Ж(|a|/g, UD/\nu). \quad (17)$$

The relation (17) is the final forms showing how the normalized vortex diameter d/$\boldsymbol{\delta}$ changes depending on acceleration and deceleration of tidal flow |a|, under the constant Reynolds number Re=DU/ν . However, it is critical to note here that the vortices appear on the sea surface only if the tidal flow is decelerated or a <$\mathbf{0}$ and absolute acceleration of tidal flow |a| exceeds to a certain threshold value.Though the acceleration a > $\mathbf{0}$ is absolutely necessary precursor of the strong vortex shedding upwards, without the following deceleration no vortices could reach at the sea surface.

LABORATORY EXPERIMENT

Objectives

The laboratory experiment is planned to examine vortex motions which occur in aflow over a series of dunes on the sea bed. A number of authors (e.g., Dyer, 1970) have measured the mean, and fluctuating velocities over gentle undulate dunes on thesea bed or in the laboratory flume

(Nezu & Nakagawa, 1993), but no measurement hasbeen conducted for the possible transverse velocity field due to vortex motions induced by the dunes, but few measurements have been made over dunes as steep as those observed in Western Port, Australia.

To enable the details of any secondary motion to be determined, flow visualizationboth within the body of water above the dunes and right on the surface of the dunes is essential. Pressures, which would be useful to explain the dynamics of the flow,could be measured without disturbance at any solid boundary, as reported by Nakagawa (1980, 1981). To facilitate the flow visualization and to reduce the variability of experimental results, it is decided to tow a series of model dunes througha tank filled with still water, thus avoiding the unwanted effects of turbulence which would be generated by the flow of the running water in a conduit.

Experimental Apparatus

The experiments are conducted in a towing tank 14.6 m long, 616 mm wide and 350mm deep. The tap water is filled until 300mm in deep at first. Then, each of the modeldunes is mounted on a false bed in the water tank, which is towed by means of a variable speed motor and cable system, as depicted in Fig. 11.

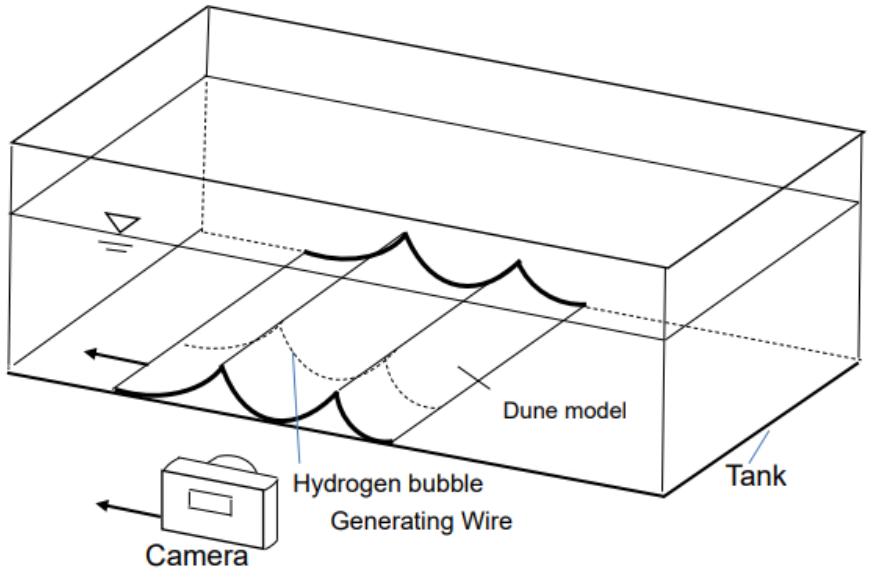

Fig. 11 Schematic diagram of towing tank experiment

The false bed was short so as to avoid generation of thick boundary layer, thus concentrating on the effects of dune model rather than on those due to the shear in the flow above them.

Several shapes of the dune model are used; in each case two identical dunes are mounted transversely to the longitudinal axis of the tank. The four shapes are depicted in Fig. 12 and their dimensions are given in Table 2.

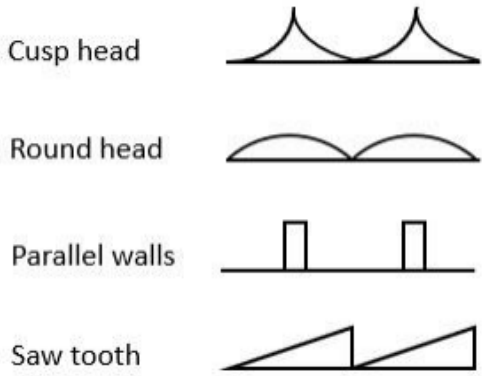

Fig. 12 Profiles of dune models.

Table 2 Dimensions of dune models

Profile	Wavelength (mm)	Wave Height (mm)	Steepness of dune
Cusp head 1	100	50	0.5
Cusp head 2	62.5	31.25	0.5
Cusp head 3	43.5	21.75	0.5
Cusp head 4	100	30	0.3
Round head	80	28	0.35
Parallel walls	100	50	0.5
Saw tooth 1	100	30	0.3
Saw tooth 2	100	10	0.1

The flow around each dune model is visualized using hydrogen bubbles generated on a copper wire of 0.08 mm in diameter located in the central vertical plane of the tank, as shown in Fig.11. Photographs were taken from the side through the transparent glass window by using a camera mounted on the carriage towed with the dune model, in the field of view illuminated by a synchronized stroboscope. The natural buoyant rise of the hydrogen bubbles is detected, butit is realized that this effect does not hinder from determining the details of the flow field in the uncorrected photographs. The flow on the direct surface of the dune model is visualized using a shallowpool of milk placed on the trough between the dunes, and is photographed from above. The experimental conditions are summarized in Table 3, where they are compared with those in the field. It will be easily noted that the flow patterns observed over the model under accelerated and/or decelerated conditions differ *markedly* from those under conditions of steady motion. Experimental parameters of laboratory experiment are not exactly same as those of field experiment, but at least comparable ones are carefully selected to avoid the violation of the similarity law for the flow (Zierep 1982), though the Reynolds numbers in laboratory experiment is smaller than those in field experiment by twoorders of 10^2.

Table 3 Comparison of experimental conditions between field and laboratory.

	Field experiment	Laboratory experiment
Velocity U (mm/s)	510	3.3 to 109.3
Acceleration α (mm/s^2)	0 to 0.	0.3 to 9.4
Deceleration $-\alpha$ (mm/s^2)	0 to -0.47	-0.3 to -9.4
Non-dimensional acceleration α/δ	0 to 4.80×10^{-5}	3.06×10^{-5} to 9.59×10^{-4}
Non-dimensional deceleration $-\alpha/\delta$	0 to -4.80×10^{-5}	-3.06×10^{-5} to -9.59×10^{-4}
Normalized acceleration π_4	0 to 3.25×10^{-2}	7.53×10^{-3} to 2.59×10^{2}
Normalized deceleration $-\pi_4$	0 to -3.25×10^{-2}	-7.53×10^{-3} to -2.59×10^{2}
Reynolds number Re	7.30×10^{6}	3.30×10^{2} to 3.01×10^{4}
Froude number Fr	3.80×10^{-2}	2.00×10^{-3} to 1.10×10^{-1}
Steepness of dune γ	0.035 to 0.190	0.1 to 0.5

Note: The normalized acceleration and/or deceleration $|\pi_4|$ is defined as $D|a|/U^2$, where D is the mean water depth, $|a|$ is the flow acceleration and/or deceleration, and U the mean velocity. The Reynolds number is defined as Re=UD/ν, where ν thekinematic viscosity. And, the Froude number is defined as $Fr=U/(gD)^{1/2}$, where g is the gravitational acceleration.

RESULTS OF LABORATORY EXPERIMENT

In performing an experimental run, each model is mounted in the still water tank, the hydrogen bubble wire is switched on, and then the camera and towing mechanism are started. Over a very short period, the towing mechanismaccelerates the model up to a constant speed which is held along the length of thetank, and finally decelerated it in a very short time, after which the hydrogen bubble wire and camera are switched off. Thus, motion of each model which may be from left to right and vice versa, consists of the following three stages:

1. Acceleration stage,
2. Constant speed stage, and
3. Deceleration stage.

Fig. 13 depicts a sequence of flow patterns spanning stages A, B, and C. In the description below and in Fig. 13, it is assumed that the observer is moving with the model and hence the flow will be seen, as if it approaches to a stationarydune on tank bed.

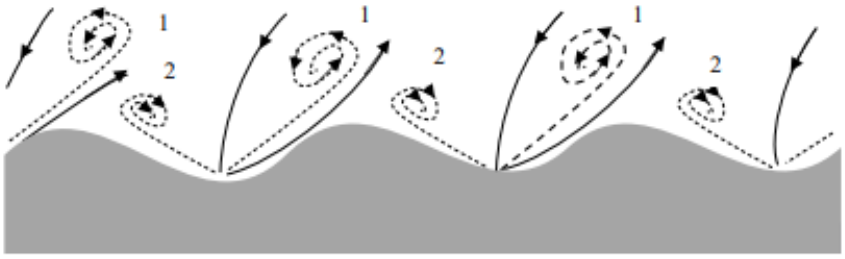

(a)

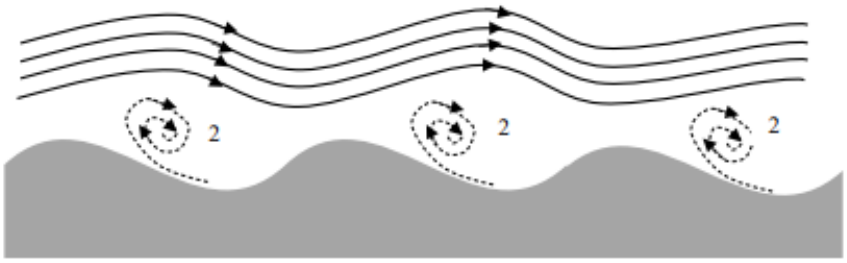

(b)

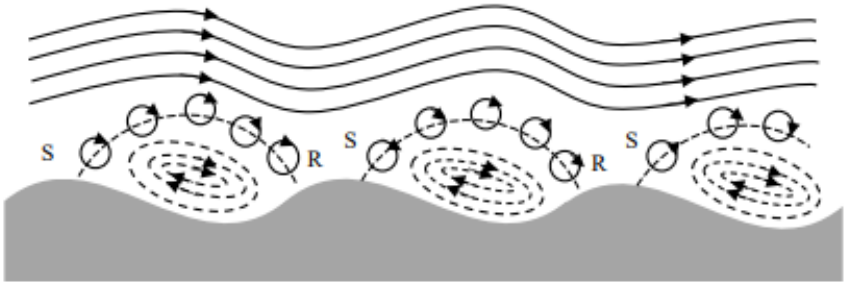

(c)

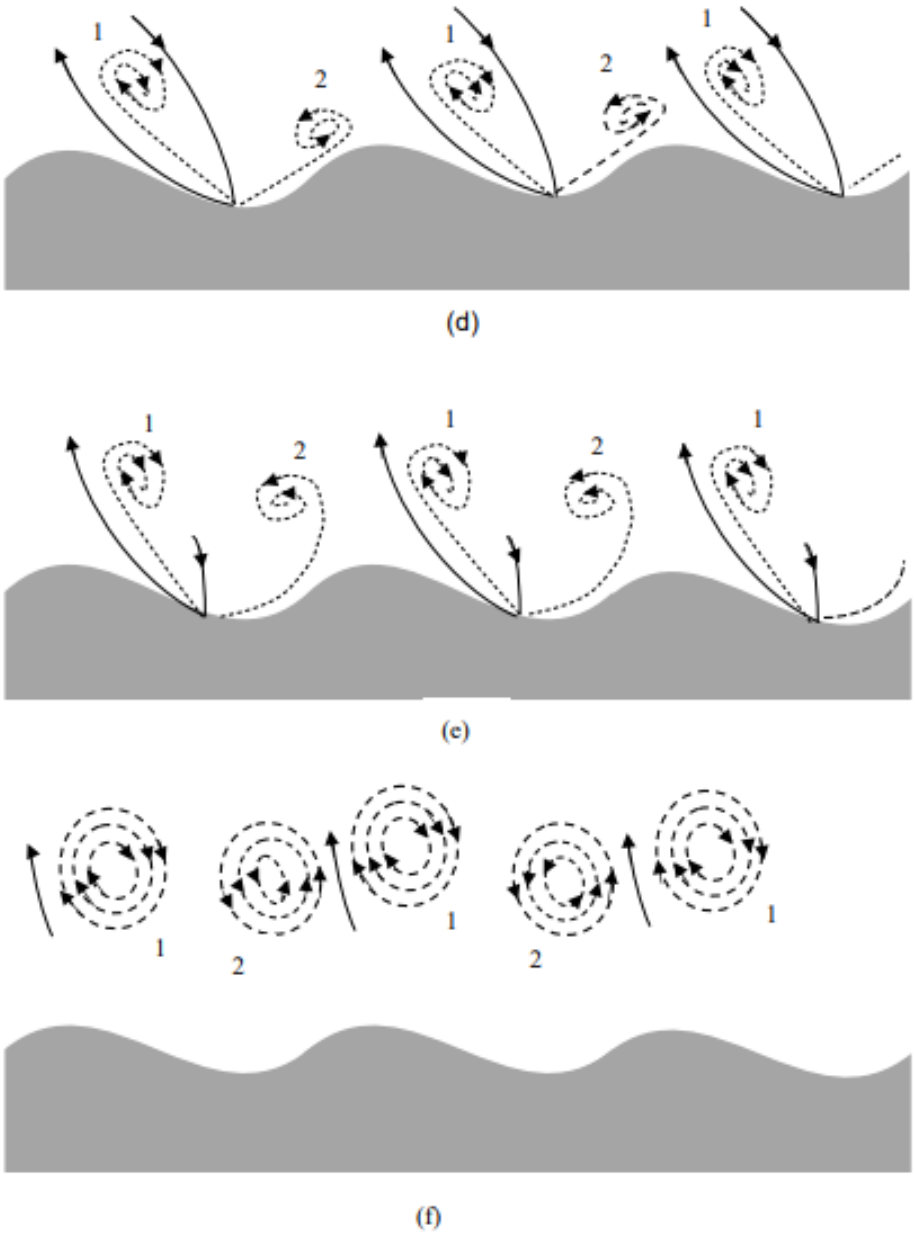

Fig. 13 A series of sketches for interaction of unsteady flow and sand dune, andresulting secondary flow and vortices. (a) and (b) show stage A with the flow starting from rest and moving from left toright; paired vortices, numbered 1 and 2 are generated, (c) shows stage B with steady flow from left to right, where letters S and R denotethe separation and reattachment points, respectively, (d), (e) and (f) show the flow evolving from steady motion to rest in stage C.

Fig. 13 (a) and (b) show stage A with the flow starting from rest and moving from left to right. Paired vortices, numbered 1 and 2, are generated. Vortex, No.1 is carried into the ambient flow, while vortex, No.2 is trapped by the bed topography and ultimately forms a separation eddy behind each dune.

Fig. 13(c) shows stage B with steady flow from left to right. Vortex No. 2 remains as the separation eddy behind each dune receives energy from the ambient flow, while it dissipates in internal and

bed shearing processes. Additional vortices of smaller dimension are formed along the dividing free streamline between vortex No.2 in the cavity and the ambient flow, and change their shape depending on geometry of the dune and the Reynolds number. The dividing free stream line may become unstable sometimes and thus some of the tiny vortices might be shed from its downstream end, viz. reattachment point R. Figs. 13 (d), (e) and (f) show the flow in stage C. As the flow decelerates, a pair of vortices is formed. These vortices move towards each crest and then are "ejected" into the ambient flow. It is certain to expect that each vortex changes into three-dimensional vortex ring directing to the water surface, in keeping an increase of the radius with time by the interaction with the sea surface (Nakagawa& Kageyama, 1977). These vortex rings may also interact with each other, by leapfrogging of the two rings for example (Yamada & Matsui, 1978).

(a) After 1 second, compare with Fig.13 (d).

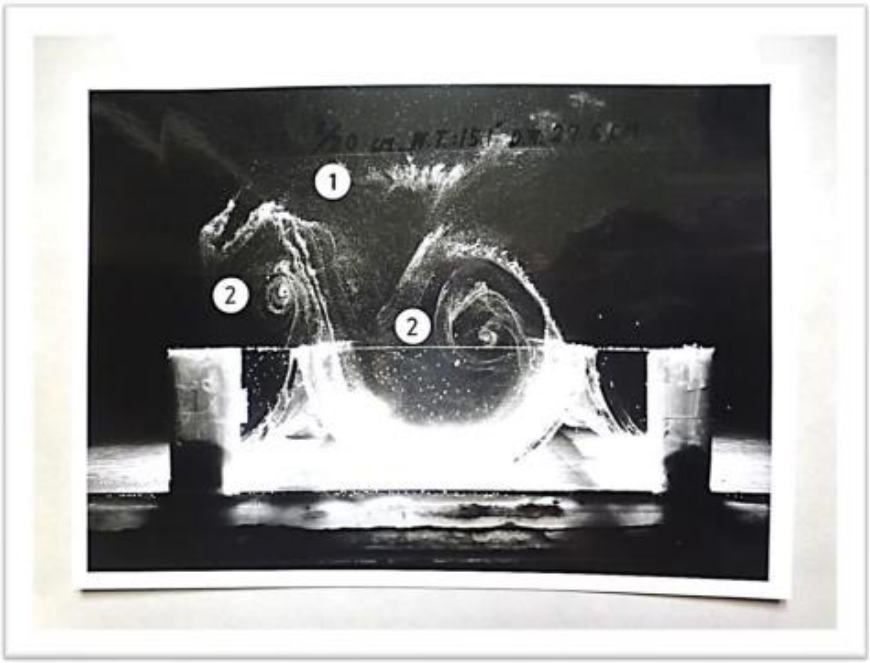

(b) After 2 seconds, compared with Fig.13 (e)

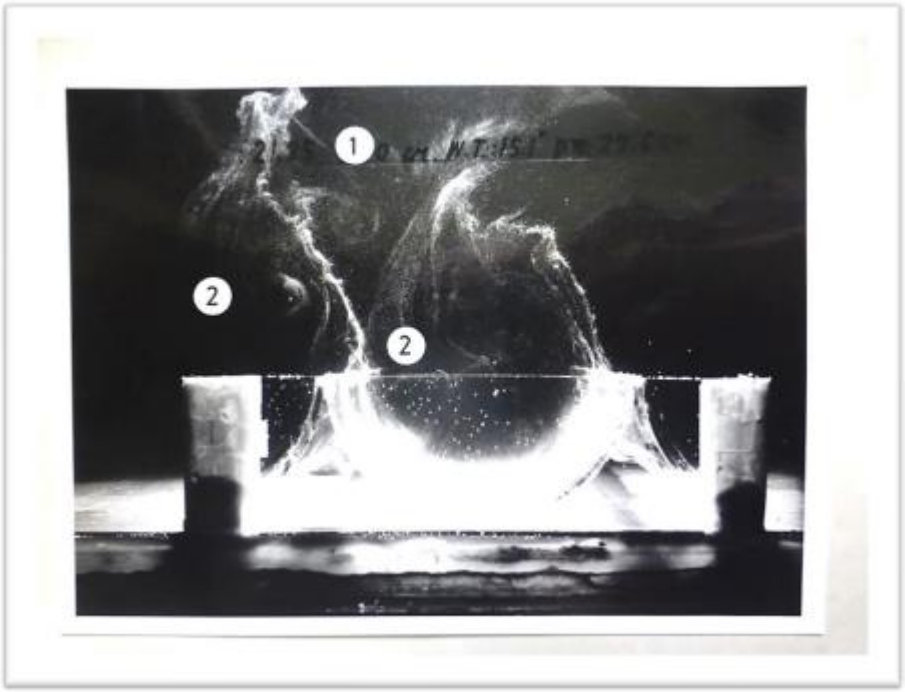

(c) After 3 seconds, compared with Fig.13 (f).

Fig. 14 Vortices generated at each crest of cusped dune model when the mainflow is decelerated at the normalized deceleration π_4=−3.13.

Figs. 14 (a), (b), and (c) correspond to Figs. 13 (d), (e), and (f), respectively, andshow the ejection of the paired vortices and their subsequent increase in cross- sectional area. Figs. 14 (a), (b), and (c) are taken at 1, 2, and 3 seconds, respectively, after the start of deceleration of a steady flow velocity, U=30 mm/s atthe normalized deceleration π_4=−3.13.

The pressure measurements made around the circumference of the dune profile have been described by Nakagawa (1980, 1981), who has confirmed the existence of a stagnation point, and directions of the motion by the hydrogen bubble flow visualization.

The flow visualization near the surface of the dune models, made by using milk, is described by Nakagawa & Hinwood (1978). They reveal a more complex and finer scale of vortices with axes aligned in the direction of primary flow. These Görtler vortices are formed by a Rayleigh-Taylor instability of the flow (Nakagawa1979b), as it passes near part of the concaved surface of a dune, as depicted in Fig.15.

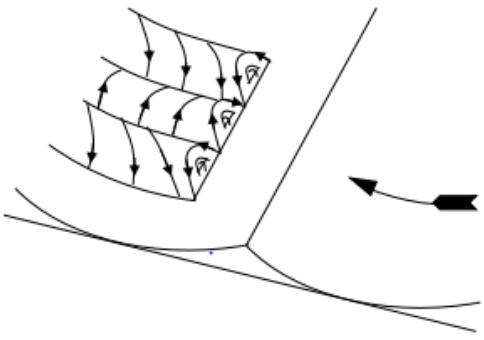

(a) Onset of Görtler Vortices

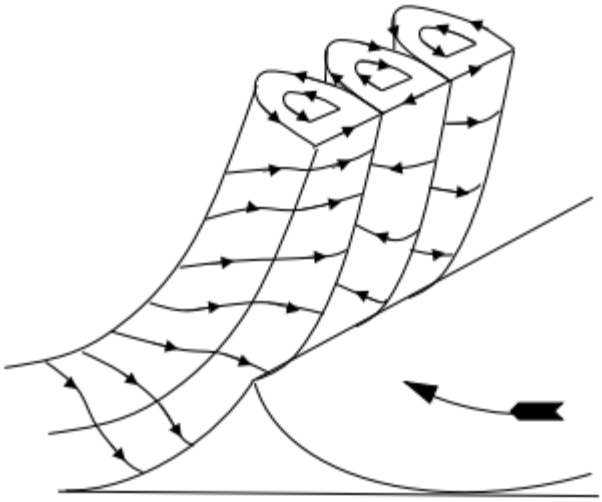

(b) Ejection of Vortices

Fig. 15 Onset of Görtler vortices and the ejection from crest of the concaved wallwhen the flow is decelerated.

The infant Görtler vortices are initially much smaller in scale than the dimensions of each dune as well as the vortices at the water surface in the laboratory water tanks or in the tidal estuaries. However, considering the potential rapid growth of the upwards ejected vortices after being pinched off (Nakagawa & Kageyama, 1977), these Görtler vortices must be a plausible candidate as the source of the large-scale vortices observed on the sea surface atWestern Port, Australia and many other spots such as river mouth and/or tidal estuary in the world. The milk flow visualization indicates that the flow normallyseparates from the dune model if the crest has a cusp, or if steepness of the dune $\boldsymbol{\gamma}$ exceeds to the value of ca. 0.1.

The same features of the secondary vortex motion are observed in the experimental runs using the other dunes although in case of the parallel walls and saw tooth shapes, additional transverse vortices are generated at corners formedby the dunes and the bed plate. In particular, in the case of the parallel walls, several vertical columnar vortices are regularly formed on the trough between two walls aligned in the transverse direction normal to the primary flow.

ORIGIN OF THE LARGE-SCALE VORTEX MOTIONS IN TIDAL CURRENTS

Possible Mechanisms

Before the laboratory results are applied to the field problem, the possible mechanisms which might be responsible for the origin of the large-scale vortex motions will be considered. It is worth reiterating that sometimes these vorticeshave been observed even above a plane smooth sea bed, so that it is probable that no single explanation can account for all examples of cellular vortex flow which have been observed in the field.

A number of possible mechanisms, which have been considered briefly by Hinwood (1978) will be reexamined here in sufficient detail to make their acceptance or rejection enable. These mechanisms are:

A. Hydrodynamic instability in a statically unstable stratified flow,
B. Instability of a statically unstable flow (thermal Bénard convection),
C. Secondary motions driven by wind shear (Langmuir cell),
D. Eddy shedding at channel bends or islands, and changes in plan form,
E. Secondary motion generated by wind waves,

F. Turbulent bursting phenomena in boundary layer flow,
G. Local imbalance in the turbulent kinetic energy budget, and
H. Interaction of tidal currents and sand or rock dunes on sea bed.
I. Other features of real flows which may give rise to disturbances, but for whichno coherent mechanism can be formulated are:
J. Variations in boundary roughness in the longitudinal and transverse directions,
K. Large scale curvature of the flow in plan, as noticed in the Gulf Stream or theKuroshio (Greenspan, 1969; Nakagawa 2019),
L. Large scale variations in mean water depth of the flow in the longitudinal andtransverse directions,
M. Large scale variations in the intensity and direction of wind shear stress during Cyclone (Hurricane or Typhoon).

The mechanisms in the first list, A-H, will be considered in the following sections, whereas the features of the flow in the second list, I-L will not be considered further as it has not been possible to develop a mechanism of generation for large-scale vortices in tidal currents based on them.

A. Hydrodynamic Instability in a statically unstable stratified Flow

Within a sharply or continuously stratified flow, instabilities may grow through a number of mechanisms. Internal waves may be present and these may be amplified by the conditions of flow, so that eventually they break. Alternatively,turbulent or other fluctuations in the flow may propagate across or along a densitygradient and may persist or may be diminished by the flow. Finally, the nature ofthe stratification would change by producing a static instability, as is observed inthe ocean under conditions resulting salt fingering.

The observation reported in the preceding section show that the sea water in which secondary vortex motions have been observed are homogeneous, eliminating the possibility of occurrence of any of these instabilities or secondary motions. However, it must be pointed out that the measurements have a certainresolution or accuracy, and that temperature (Fig.7) or salinity (Fig.8) differences smaller than that resolution are present. Even such very weak stratifications in flows of high Reynolds numbers would cause to let perturbations be unstable across a wide span of wave numbers (Shlichting, 1935; Turner, 1973). Thus, the turbulence generated within the tidal current may be possible to penetrate this stratification and would lead to effective mixing. Nonetheless, there appears tobe no mechanism by which the present cellular vortex motions can have arisen ina statically stable stratified flow.

B. Instability in a statically unstable Flow (Thermal Bénard Convection)

The present vortices bear some resemblance to the Bénard cells (Chadrasekhar, 1961), which are formed when a horizontal viscous fluid layer is either heated from below or cooled from above. This heating or cooling producesa static instability which drives the secondary motion to form hexagonal cells distributed over the surface. Although the classical description of the Bénard cells relates to the case of heating of an initially stationary fluid confined betweenparallel horizontal plates, many other cases have been examined including heatingfrom below of a flowing fluid with a free upper surface, a case resembling the geometry of the present flow.

The temperature data (Fig.7) and the argument presented in the preceding section would appear to eliminate this mechanism from further consideration. Itwas considered that a surface layer of water a few millimeters in thickness might have been cooled by evaporation or other heat loss to the

atmosphere, and thus in this very thin layer certain secondary motions could be observed. To test thishypothesis, water was collected by lowering several vessels a few millimeters below the sea surface at the test site, and allowing them to fill by skimming the surface layer. No temperature difference was observed between the water in the different vessels or between that water and the water in the rest of the vertical profiles at any section of measurement. Hence, this possible mechanism must be eliminated from further consideration.

C. Secondary Motion driven by Wind Shear (Langmuir Cell)

Secondary motion known as the Langmuir cells (Langmuir, 1938) is caused bythe shear stress exerted on the sea surface by the wind.

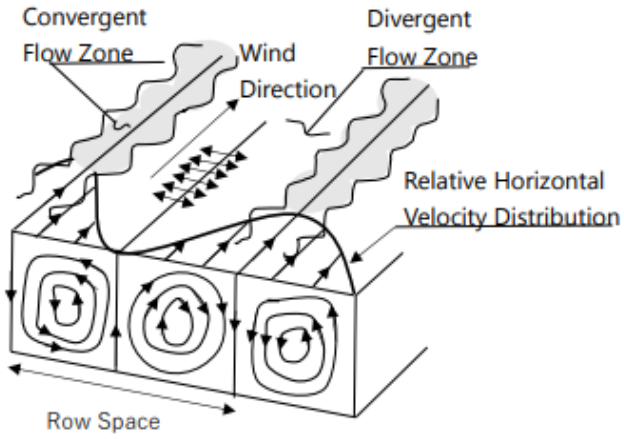

Fig. 16 Hypothetical sketch of Langmuir circulation

As depicted in Fig.16, the Langmuir cells are helical vortices with axes alignedin the primary wind direction, in which each vortex has a sense of rotation opposite to that of the adjacent vortices. It is conceivable that long vortices of this kind would be broken up in shallow to form the roughly elliptical cells like rugby ball observed in the field experiments [see Figs. 4 (a) and (b)]. However, the Langmuir cells have been observed in the field only when the wind speed exceeds about 3 m/s, while the present cellular vortex motions have been observed most frequently when the wind speed is below 1 m/s, including some observations under calm conditions. Thus, it can be concluded that the Langmuir cells are not the prime mechanism of generation of the present cellularvortex motions, although it is possible that wind shear could play certain role in some occasions.

D. Eddy Shedding at Channel Bends or Islands and Changes in Plan Form

It is frequently observed that eddies are periodically shed in the wake of aheadland or in the downstream from a bend in tidal estuaries. It is evenconceivable that these eddies would tend to generate counter-rotating eddies inthe adjacent water, giving rise to a field of eddies. The eddies are supposed tobe generated by the mean flow, so that the total head of the fluid comprising theeddies will remain approximately the same as that of the mean flow. It is certainthat in addition to the internal shear stress dissipation both the mean flow and thesuperimposed eddy motion will lose energy due to shear stress on the sea bed aswell as the boundary of land or island. Data obtained by Hinwood & Jones(1979)show that this loss may be described by use of the velocity profile, $U/U^*=2.5\cdot\ln(y/z_0)$, where U is the mean velocity of tidal current, U^* is the friction velocity, and z_0 is the height scale at height y above the bed. Moreover, the Chézy coefficient, is defined as

$C=U/(mr)^{1/2}=28 \cdot D^{1/6}$ in S.I. units, where m is the hydraulic mean radius, r is the specific gravity of sea water, and D is the water depth of 18 m in the present measurements. The kinetic energy of the mean motion is maintained bythe water surface slope arising from the tidal rise and fall, but there is no comparable process sustaining the eddy motion, which will thus start decaying immediately after its generation. It may be seen from Fig.2 that the test site is approximately 8 km from the nearest promontory likely to shed eddies. The rate of decay of the total head of the eddy motion is estimated, and the total head will decay to 1.3 % of the initial value. Any generation of additional subsequent eddies must increase the rate of extraction of energy from the initially-generated eddies. However, no energy is available for generating the strong, regular vortex motions.

From these considerations, it appears most unlikely that eddies shed from plan-form features of the channel could give rise to strong, regular vortex motionssuch as those observed.

D. Secondary Motion generated by Wind Waves

In this regard, two possible mechanisms might be considered. Firstly, the direct production of vortex motion by the waves could be considered. This possibility may be dismissed as no other observers have seen vortex motions of the present kind induced by waves. Furthermore, on some occasions when waves are present the wavelengths differed from the vortex dimensions and the waves sometimes in the direction of the tidal current and at other times in other directions, making it difficult to see how energy could be transferred to a vortex motion.

The second possibility is that the oscillatory motion of the water, caused by thewaves, interacts with the rock or sand dunes on the sea bed in the way demonstrated by the laboratory experiment in the preceding section. On the days when field data were obtained, the wind was slight and wavelengths produced by the wind were only a few meters long. Thus, the ratio of the water depth to the wavelength was much greater than twice, and hence the waves may be regarded as deep-water waves with a minimum interaction with the sea bed. Furthermore, the period of these short water waves was typically about two seconds, which is much less than the period required for a current of 0.6 m/s to advent a vortex of length 0.405 ~ 12.7 m from the bed to the sea surface.

E. Turbulent Bursting Phenomena in Boundary Layer

Kline et al. (1967) have shown that in the turbulent boundary layer on a smoothflat plate, turbulence is generated intermittently near the wall. They have also shown that the main contributors to the Reynolds stress are discrete sweep and ejection events. These events may extend well into the free stream above the boundary layer (Corino & Brodkey, 1969; Grass,1969; Gordon,1974,1975). Heathershow (1974) has suggested that the laboratory results are directly applicable to flows of geophysical scale. Gordon found that the mean non- dimensional bursting period, T^*, has a nearly constant value, $T^*=UT/\delta_1=5$, where U is the mean velocity of the fluid, T the mean bursting period, and $\delta_1 = \int^{\infty} (\boldsymbol{U} - \boldsymbol{u})\boldsymbol{dy}$, the displacement thickness of the turbulent boundary layer, where $\boldsymbol{y}=\boldsymbol{0}$ u is the flow velocity, and y is the vertical coordinate from the sea bed. This is consistent with laboratory result of Rao et al. (1989) and others. Gordon obtained the result that 99 % of the contribution to the Reynolds stress is made during only 55 % of the total time. Gordon's experiments are carried out at a maximum tidal velocity of 0.75 m/s yielding a Reynolds number based on depth ofwater of the order of 10^6 to 10^7. In the present field experiments, the maximum velocity of the tidal current is of 0.65 m/s, and the Reynolds number is $7.3x10^6$, resulting conditions comparable with those of Gordon.

If it is hypothesized that the tidal current in an estuary corresponds to a turbulent boundary layer over a flat plate, it is possible that the ejection event which is part of the bursting process produces the vortices observed at the sea surface. In favor of this hypothesis are the previously cited observations that the ejection events are produced by the mean motion and that they propagate farfrom the boundary, or sea bed. Against this hypothesis, the bursting process isthe random and intermittent nature; based on Gordon's bursting period formula, bursting events would have a mean separation of 21 m in the present flow. It is,therefore, difficult to see how the regular arrays of vortices observed in the field can be produced by the random ejection events. However, it has been observedthat the precursor of an ejection can be a weak perturbation of the outer part of the boundary layer. The possibility that this disturbance is supplied by a previously generated ejection arriving at the sea surface has been investigated byHinwood (2020), who concluded that it could not be ruled out of consideration in the case of a uniform, non-accelerated shear flow over a plane bed. A similar suggestion to this has been examined by Nezu & Nakagawa (1993), but they have unfortunately overlooked the most critical factor of the deceleration of the flow toconvey the vortices generated at the bed to the sea surface: *Vortex ejection fromthe sea surface due to bursting phenomena is considered not to have enough potential to carry vortices until the sea surface if there is no deceleration of flow.* In addition, the conditions that induce bursting phenomena are not well satisfied by the present field experiments, for the dunes on the sea bed make the application of flow over a flat plate implausible.

Additionally, it may be worth noting here that oceanic Rossby waves (Chelton & Schlax 1982, Dickinson 1970, Tyler 2008) are caused by the Coriolis force and conservation of potential vorticity which leads to change of relative vorticity. They are large-scale waves within an ocean basin, and gain momentum from windshear at the ocean surface layer with no significant vertical motion of fluid. On one hand, the planetary Rossby waves (Covey & Schubert 1982, Kospi & Schneider 2011, Shepherd 1987) are easily observed in the atmosphere as the large meanders of the mid-latitude jet stream that are responsible for prevailing seasonal weather patterns and their day-to-day variations. However, Rossby waves have been much more difficult to detect in the ocean because of their smallsea-surface signature (height variations of order 10 cm or smaller), slow propagation speeds (of order 10 cm/s or less) and long wavelengths (hundreds tothousands of kilometers).

Thus, it is evident that oceanic Rossby waves (Rossby, 1939) must be differentfrom the present vortices in appearance, origin and generation mechanism.

F. Local Imbalance in the turbulent kinetic Energy Budget

Talke et al. (2013) have investigated the relationship between turbulent statistics and coherent structures in an unstratified reach of the Snomish River estuary in USA, using in situ velocity measurement and surface infrared imaging.Sequential infrared images are used to estimate surface flow characteristics via aparticle image-velocimetry (PIV) technique, and are conditionally sampled todelineate the surface statics of bottom-generated boils. Boils and their surfacemanifestation, therefore, play a critical role in the vertical transport of turbulent kinetic energy and the water column distribution of dissipation, and are animportant of the turbulent kinetic energy budget. Over a large, depth-scale sill,Chikadel et al. (2009) and Talke et al. (2010) have found that boils are linked to flowseparation and mixing layer growth.

Orton et al. (2010) have found that energy dissipation caused by wind-inducedshear dominates over dissipation caused by bottom-generated turbulence at a near surface measurement location (ca.50 cm below surface) in the Hudson Riverestuary in USA. Near surface, turbulence production and

dissipation are approximately equal, though a significant upward-directed turbulent-transport accompanying boils is from time to time reported during strong tidal currents at many spots in the world. Note that Scully et al. (2011) have reported that they are unequal in the lower water column in areas of high roughness on bed.

Talke et al. (2010) have studied how the growth of mixing layer (separated flow)and embedded coherent structures to be developed into boils eventually, are influenced by the surface boundary more strongly as water depth over a sill decreases. On the contrary, they conclude that the surface significantly damps growth of coherent structures and inhibits to form boils once the sill height exceeds to ca.80% of the local water depth.

Moreover, Talke et al. (2013) adopt a unique research platform that couples infrared remote sensing of the water surface in order to identify the detailed surface expression of boils, together with highly being resolved and collocated near-surface and water column turbulence measurements below the surface. This remarkable combination enables them to quantitatively link the subsurface turbulent structure with its surface expression, boils, and to measure the turbulent kinetic energy $q^2=\langle u'^2\rangle+\langle v'^2\rangle+\langle w'^2\rangle$, where u′, v′ and w′ are x, y and z fluctuation components of the velocity, respectively, and its dissipation rate ε within boils. They show that boils are low-momentum water masses with elevated turbulent kinetic energy and vertical velocity variance, which is the mean of the squares of deviations of the data values at the data set, relative to the ambient surface water.Boils are marked by horizontal divergence and upwelling, which may be caused by the interaction of coherent structures with the kinematic boundary condition.It may be natural to consider that downwelling also occurs at each of the boil boundaries and boundaries with the ambient flow to preserve the continuity of flow.

The turbulent kinetic energy budget in the water column indicates that production P and dissipation ε are not in balance generally. Instead, P exceedsε near the bottom of the sea and/or river; this abundant shear production of the turbulent kinetic energy well exceeds the local capacity to dissipate the energy, resulting in the local imbalance. Talke et al(2013) have hypothesized that such an excess turbulent kinetic energy is transported away only from the bottom towards the surface, though there might be no reason why the excess energy only aims atthe water surface. It may be evident that the excess energy could moves towards the ambient locations in the same and/or even lower level as well.

It is plausible that the water surface suppresses the vertical motions with a scalegreater than the depth H, but admits smaller, boil-scale motions. It is therefore clear that a marked scale dependence of statistical isotropy develops, with anisotropic conditions observed near the surface for scales greater than the depthH, and approximately equal and horizontal velocity variance may be observed at scales equal to or smaller than the boil scale. Such statistically isotropic conditions are governed by the spatial structure of the surface, which contains patchy boils consisting of many regions of upwelling and downwelling.

G. Interaction of tidal Currents and Sand Dunes

The laboratory experiments reported in preceding section have shown that decelerated flow over steep, sharp-crested dunes will lead to the vortices, and thatthese vortices may propagate upwards into the body of the flow.

The range of steepness of the sand dunes in Western Port, Australia was 0.035to 0.19, while the experiments have shown that the flow separation is likely to occur if the steepness $\boldsymbol{\gamma}$ is greater than 0.1, as it is in the model experiments (Table3). However, it is also found that the flow separated at the sharp crest of each of saw tooth profile dune models which must be a good approximation to the real dune on the sea bed. Thus, the model flow patterns are likely to berepresentative of those in the field, and hence a decelerating tidal current flowing over the sand dunes could produce the paired vortices at the crest of each dune. The similitude analyses revel the fact that the normalized deceleration $-\boldsymbol{\pi}_4$ in the laboratory experiments covers that in the field experiments. In addition, the Reynolds number Re, the Froude number Fr, and the steepness of dune $\boldsymbol{\gamma}$ in the laboratory experiments are comparable in order with those in the field experiments, as being evident in Table 3.

It is critical to note that cellular vortices have only been observed close to the time of tide when the current velocities record a maximum and hence close to the singular time when the acceleration flow changes to deceleration one. This flow change from acceleration to deceleration coincides with the condition of Fig. 14(b),in which paired vortices are ejected into the ambient flow from the crest of each dune. Although the magnitude of the deceleration in the field is less than that in the laboratory experimental runs, but it is revealed by the present similitudeanalyses that the order of the normalized deceleration characteristic number $-\boldsymbol{\pi}_4$ is the same. It is, therefore, suggested that the occurrence of the vortex ejectionis primarily governed by degree of the deceleration in tidal current: The critical point in this regard is whether the vortex is ejected upwards or not, depends on acceleration and deceleration of the tidal current, and its magnitude is increased as the higher degree of acceleration and deceleration in the current! The precursor acceleration plays a decisive role in enhancing the strong upwards ejection of vortex being assisted by the following deceleration of the tidal current. This may the main reason why the Uzushio or large-scale vortices are often observed on the sea surface during the spring tide, where just before the flood the accelerationreaches at the maximum, and then after the flood the deceleration becomes at themaximum. It is certain that during the acceleration period fluid dynamicalenergy is accumulated in the cavity behind dunes, and the energy would be released upwards in a form of vortex once the deceleration of flow begins.

On the basis of the present findings, as well as the existing information andknowledge (Nakagawa & Kageyama,1977), a tentative kinematic model of the large-scale vortex motion in strong tidal current is elaborated as a tentative hypothesis: After being ejected from the crest of each dune on the sea bed into the ambient flow, the vortex moves to the sea surface, experiencing a series of changes in its structure. Though the present proposed processes from the sea bed to the surface have not been verified quantitatively yet, it may be evident thatnear the sea surface, the vortex grows the diameter with moving upwards by entraining the surrounding water and by the strong interaction with the sea surface.

Further evidences for the mechanism proposed are firstly the agreement in thepeaks on the vortex-diameter frequency distribution, Fig. 5, and dune-scale frequency distribution, Fig. 10, and secondly the existence of upwards flow in thecenter of each vortex, which has been revealed by the flow visualization experiment in terms of dye patches. The evidences available thus support the hypothesis that an interaction between the tidal flow and the dunes generates the vortices (or boils) and the acceleration and deceleration of the tidal currents couldplay a decisive role in ejecting the paired vortex, to be transported to the sea surface eventually.

CONCLUSIONS

In this section, new knowledge and insights obtained through the presentstudy have been summarized. It is concluded that the present vortices are generated by the interaction of tidal currents and sand dunes at one singular time during spring tide: When tidal currentschange from acceleration to deceleration, the fluid body in the re-circulatory flow region (cavity) behind each dune is transformed into a pair of vortices. Then, the paired vortices are ejected to the sea surface in experiencing a series of changes in vortex structure, and finally form the cellular vortices on the sea and/or river surface. It is found that interaction of the tidal currents and the sand dunes on sea bed appears most likely to have generated the infant Görtler vortices, which evolved into the large-scale vortices at the sea surface eventually. It is realized that the large-scale cellular vortices provide significant influence onthe vertical transport of material, such as effluent, and hence will exert a major influence on longitudinal dispersion in the sea. Vertical momentum transport inthe upper part of the flow will also be profoundly altered by the vortices. It is inferred that the present findings are critical to understand any oscillating flow innature and laboratory accompanying the cyclical change from acceleration to deceleration and vice versa. In addition to tidal current, any oscillating flow such asflow in blood vessel, and/or in a wave, must be relevant to the present study.

ACKNOWLEDGEMENTS

The present work is conducted as principal part of the junior author's Ph. D study in the Department of Mechanical Engineering, Monash University, under the supervision of Dr. Jon B. Hinwood, who has been the immobile leader for this projectover the last half-century. Paying authors' profound respect to his resilient work, thispaper has been cordially dedicated to Dr. Hinwood. This work is supported by Monash Graduate Scholarship and Grant No.H74/15520 of the Australian Research Grants Committee.

REFERENCES

Best, J. (2005a), The fluid dynamics of river dunes: A review and some futureresearch directions, J. Geophys. Res., 110, F04S02, doi:10.1029/2004JF000218. Best, J. (2005b), Kinematics, topology and significance of dune-relatedmacroturbulence: Some observations from the laboratory and field, Spec. Publ. Int. Assoc. Sedimentol., 35, 41–60.

Branch, R.A., A. R. Horner-Devine, A.R., Chickadel, C.C., Talke, S.A., Clark, D., Jessup, A.T. (2021) Surface Turbulence Reveals Riverbed Drag Coefficient, Geophysical Research Letters, 10.1029/2020GL092326, 48, 10.

Chandler, B., Berzkalns, E. (1977) Turbulence in tidal currents. B. Eng. Thesis, Department of Mechanical Engineering, Monash University.

Chandrasekar, S. (1961) Hydrodynamic and Hydro-magnetic Stability, Oxford University Press, p.10.

Chelton, D.B. Schlax, M.G. (1996) Global observation of oceanic Rossby waves. Science, 272, 234-238.

Chickadel, C. C., Horner-Devine, A. R., Talke, S. A., Jessup, A. T. (2009), Vertical boil propagation from a submerged estuarine sill. Geophys. Res. Lett., 36, L10601, doi:10.1029/2009GL037278.

Corino, E.R., Brodkey, R.S. (1969) A visual investigation of the wall region in turbulentflow. J. Fluid Mech. 37, 1-30. 39, no.11.

Covey, C., Schubert, G. (1982) Planetary-scale waves in the Venus atmosphere. J. Atmos. Soc. 39(11), 2397-2413.
Daniel R. Parsons, D. R., Best, J. (2013) Bedforms: views and new perspectives from the third international workshop on Marine and River Dune Dynamics (MARID3). Earth Surface Processes and Landforms, 10.1002/esp.3360, 38, 3, (319-329).

Darrigol, O. (2005) Worlds of Flow-A History of Hydrodynamics from the Bernoulli toPrandtl. Oxford University Press, Oxford, p.154.

Dickinson, R.E. (1978) Rossby waves-long-period oscillations of oceans andatmospheres. Ann. Rev. Fluid Mech. 10, 159-195.

Dyer, K.R. (1970) Current velocity profiles in a tidal channel. Roy. Astron. Soc. Geophys. J. 22, 153-161.

Gakhar, S., Koseff, J. R., Nicholas T. Ouellette, N.T. (2020) On the surface expression of bottom features in free-surface flow. J. Fluid Mech., 10.1017/jfm.2020.548, 900.

Gakhar, S., Koseff, J. R., Nicholas T. Ouellette, N.T. (2022) Extracting free-surfaceexpressions of underwater features. Experiments in Fluids, 10.1007/s00348- 022-03491-w, 63, 9.

Gordon, C.M. (1974) Intermittent momentum transport in a geophysical boundary layer. Nature, 248, 392-394.

Gordon, C. M. (1975) Period between bursts at high Reynolds number. Phys. Fluids,18, 141-143.

Grass, A.J. (1971) Structural features of turbulent flow over rough and smoothboundaries. J. Fluid Mech. 50, 233-255.

Greenspan, H.P. (1969) The Theory of Rotating Fluids. Cambridge at the UniversityPress, London, pp. 328.

Heathershaw, A.D. (1974) "Bursting" phenomena in the sea. Nature, 248, 394-395. Hinwood, J.B. (1978) Large-scale turbulence in tidal currents.Proc. 16th Int. Conf. on Coastal Eng. Hamburg, Aug. 1978, 2598-2601.

Hinwood, J.B. (2020) A turbulent burst model of a tidal current.Privatecommunication.

Hinwood, J.B., Jones, J.C.E. (1979) Hydrodynamic data for Western port, Victoria.Marine Geol. 30, 47-63.

Kino, T. (1912) The Tosa Nikki（土佐日記） pp.128. (In Japanese)

Kline, S., Reynolds, W.C., Schraub, F.A., Runstadler, P.W. (1967) The structure ofturbulent boundary layers. J. Fluid Mech. 30, 741-773.

Kospi, Y., Shneider, T. (2011) Winter cold of eastern continental boundaries induced bywarm ocean waters. Nature, 471, 631-634.

Kostaschuk, R. A., Church, M.A. (1993), Macroturbulence generated by dunes:Fraser River, Canada. Sediment. Geol., 85, 25–37.

Langmuir, I. (1938) Surface motion of water induced by wind. Science, 87, 119-123.

Mandel, T.L., Rosenzweig, I., Chung, H., Nicholas T. Ouellette, N.T., Koseff, J.R.(2017) Characterizing free-surface expressions of flow instabilities by tracking submerged features. Experiments in Fluids, 10.1007/s00348-017-2435-6, 58, 11. Müller, A., Gyr, A. (1986) On the vortex formation in the mixing layer behind dunes, J. Hydraul. Res., 24, 359–375.

Nakagawa, T. (1979a) On flow and flow instability over concave walls with reference tosedimentation. A thesis submitted to the Faculty of Engineering in partial fulfilment of the requirement for the degree of doctor of philosophy, Department ofMechanical Engineering, Monash University, Clayton, Victoria, Australia

Nakagawa, T. (1979b) Columnar vortices in cavity flow. Naturwissenschaften, 66, 468-469.

Nakagawa, T. (1980) A device for measuring a low-pressure difference. Trans. ASME, J. Fluid Eng. 102, 499-501.

Nakagawa, T. (1981) On flow and pressure distribution around solid dune models. Proc. 25th Japanese Conf. on Hydraulics, Tokyo, Feb. 1981, 47-54. (In Japanese).

Nakagawa, T.R.M. (2019) Universal thesis of meanders. Social Sci J. 4, 153-166. Nakagawa, T., Kageyama, S. (1977) On the growth and breakdown of vortex rings.

Memoirs of the Defense Academy, Japan, Vol. XVII, No.1, 45-54.

Nakagawa, T., Hinwood, J.B. (1978) A proposed model of large-scale cellular motion instrong tidal flows. Proc. 4th Aust. Conf. on Coastal and Ocean Eng. Adelaide, Nov.1978, 185-189.

Nezu, I., Nakagawa, H. (1993) Turbulence in Open-Channel Flows. IAHR Monograph, A. A. Balkema, Rotterdam, pp.286.

Osonphasop, C. (1983) The measurements of turbulence in tidal currents. A thesis submitted to the Faculty of Engineering in partial fulfilment of the requirement for the degree of doctor of philosophy, Department of Mechanical Engineering, Monash University, Clayton, Victoria, Australia.

Osonphasop, C., Hinwood, J.B. (1983) Turbulence measurements for the whole depthof water in a tidal channel. 8th Australasian Fluid Mechanics Conference, University of New Castle, September 5, 10A, 10-14.

Osonphasop, C., Hinwood, J.B. (1984) On measurement of turbulence and shear stresses in tidal currents. APD-IAHR 4th Conference of the International Association for Hydraulic Research, Chiang Mai, May 25, 1984, 5B, 1-5.

Osonphasop, C., Nakagawa, T.R.M. (2014) Novel power law of turbulent spectrum.

Open Journal of Fluid Dynamics 2014. http://www.scirp.org/journal/ojfd Pollock, T.J. (1973) A water quality model for Western Port Bay, M. Eng. Sc. Thesis, Department of Mechanical Engineering, Monash University.

Rao, N.K., Narashimha, R., Narayanan, M.A. (1971) The 'bursting' phenomenon in a turbulent boundary layer. J. Fluid Mech. 48, 339-352.

Rossby, C.-G. (1939) Relation between variations on the intensity of the zonal circulation of the atmosphere and the displacements of the semi-permanent centersof action. J. Marine Res. 2, 38-55.

Shepherd, T.G. (1987) Rossby waves and two-dimensional turbulence in a large-scalezonal jet. J. Fluid Mech. 83, 407-509.

Schlichting, H. (1935) Tunbulenz bei Wärmeschichtung. Z. Ange. Math. Mech. 15, 313-338.

Scully, M.E, Geyer, W.R., Trowbridge, J.H. (2011) The influence of stratification andnonlocal turbulent production on estuarine turbulence: An assessment of turbulence closure with field observations. J. Phys. Oceanogr. , 41, 166-85.

Talke, S.A., Horner-Devine, A.R., Chickadel, C.C. (2010) Mixing layer dynamics in separated flow over an estuarine sill with variables stratification. J. Geophys.Res., 115, c09004, Wiley Online Library ADSWeb of Science®Google Schol

Talke, S.A., Horner-Devine, A.R., Chickadel, C.C., Jessup, A.T. (2013) Turbulent kinetic energy and coherent structures in a tidal river. J. Geophys. Res.: Oceans, 10.1002/2012JC008103, 118, 12, (6965-6981).

Tyler, R.H. (2008) Strong Ocean tidal flow and heating on moons the outer planets. Nature, 456, 770-772.

Turner, J.S. (1973) Buoyancy Effects in Fluids. Cambridge University Press, pp.367.

Venditti, J. G., Bauer, B.O. (2005) Turbulent flow over a dune: Green River,Colorado, Earth Surf. Processes Landforms, 30, 289–304.

Yamada, H., Matsui, T. (1978) Preliminary study of mutual slip through a pair of vortices. Physics of Fluids, 21, 292-294.

Yue, W., Lin, C.-L., Patel, V.C. (2005) Coherent structures in open-channel flowsover a fixed dune. J. Fluids Eng., 127, 858–864.

Yue, W., Lin, C.-L., Patel, V.C. (2006) Large-eddy simulation of turbulent flow overa fixed two-dimensional dune. J. Hydraul. Eng., 132, 643–651.

Zierep, J. (1982) Ähnlichkeitsgesetze und Modellregeln der Strömungslehre. Braun-Verlag, Karlsruhe. pp.146.

Zierep, J., Nakagawa, T.(1986) Similarity Law of Flow. IPC, Tokyo, pp.219.